

1 **Cassini in situ observations of long duration magnetic** 2 **reconnection in Saturn's magnetotail**

3 C.S. Arridge¹, J.P. Eastwood², C.M. Jackman³, G.-K. Poh⁴, J.A. Slavin⁴, M.F.
4 Thomsen⁵, N. André⁶, X. Jia⁴, A. Kidder⁷, L. Lamy⁸, A. Radioti⁹, D.B.
5 Reisenfeld¹⁰, N. Sergis¹¹, M. Volwerk¹², A.P. Walsh¹³, P. Zarka⁸, A.J. Coates¹⁴,
6 M.K. Dougherty²

7 1. Department of Physics, Lancaster University, Bailrigg, Lancaster, LA1 4YB, United Kingdom.

8 2. Department of Physics, Imperial College, South Kensington, London, SW7 2BW, United Kingdom.

9 3. School of Physics and Astronomy, University of Southampton, Southampton, SO17 1BJ, United Kingdom.

10 4. Department of Atmospheric, Oceanic and Space Sciences, University of Michigan, 2455 Hayward St., Ann
11 Arbor, Michigan 48109-2143, USA

12 5. Planetary Science Institute, 1700 East Fort Lowell, Suite 106, Tucson, Arizona 85719-2395, USA.

13 6. CNRS, Institut de Recherche en Astrophysique et Planétologie, 9 avenue du colonel Roche, BP 44346,
14 31028 Toulouse Cedex 4, France.

15 7. Department of Earth and Space Sciences, University of Washington, Box 351310, Seattle, Washington
16 98195, USA.

17 8. LESIA-Observatoire de Paris, CNRS, UPMC Univ. Paris 6, Univ. Paris-Diderot, 92195, Meudon, France.

18 9. Laboratoire de Physique, Atmosphérique et Planétaire, Institut d'Astrophysique et de Géophysique,
19 Université de Liège, Liège, Belgium.

20 10. Department of Physics and Astronomy, University of Montana, Missoula, MT 59812, USA.

21 11. Office for Space Research, Academy of Athens, 4, Soranou Efesiou str., 11527, Papagos, Athens,
22 Greece.

23 12. Austrian Academy of Sciences, Space Research Institute, Schmiedlstraße 6, 8
24 042 Graz, Austria.

25 13. Science and Robotic Exploration Directorate, European Space Agency, ESAC, Villanueva de la Cañada,
26 28692 Madrid, Spain.

27 14. Mullard Space Science Laboratory, Department of Space and Climate Physics, University College
28 London, Holmbury St. Mary, Dorking, Surrey, RH5 6NT, United Kingdom.

29 **First paragraph**

30 Magnetic reconnection is a fundamental process in solar system and astrophysical
31 plasmas, through which stored magnetic energy associated with current sheets is
32 converted into thermal, kinetic and wave energy¹⁻⁴. Magnetic reconnection is also thought
33 to be a key process involved in shedding internally-produced plasma from the giant
34 magnetospheres at Jupiter and Saturn through topological reconfiguration of the magnetic
35 field^{5,6}. The region where magnetic fields reconnect is known as the diffusion region and in
36 this paper we report on the first encounter of the Cassini spacecraft with a diffusion region
37 in Saturn's magnetotail. The data also show evidence of magnetic reconnection over a
38 period of 19 hours revealing that reconnection can, in fact, act for prolonged intervals in a
39 rapidly-rotating magnetosphere. We show that reconnection can be a significant pathway
40 for internal plasma loss at Saturn⁶. This counters the view of reconnection as a transient
41 method of internal plasma loss at Saturn^{5,7}. These results, whilst directly relating to the
42 magnetosphere of Saturn, have applications to understanding other rapidly rotating
43 magnetospheres, including that of Jupiter and other astrophysical bodies.

44 **Main**

45 Since the discovery of H₂O plumes from the icy moon Enceladus it has become clear that
46 the dominant source of plasma in Saturn's magnetosphere is the ionisation of neutral
47 molecules deep within the magnetosphere, producing a plasma composed of H₂O⁺, H₃O⁺,
48 OH⁺, collectively referred to as the water group, W⁺ (8-10). Some of this plasma is lost from
49 the system by charge-exchange, the remaining plasma is transported radially outward.
50 The radial transport is driven by the centrifugal interchange instability, which is analogous
51 to the Rayleigh-Taylor instability with gravity replaced by the centrifugal force associated
52 with the rapid rotation of the magnetosphere⁶.

53 Magnetic reconnection is a process involving topological rearrangement of the magnetic
54 field. Generally this involves either connecting planetary magnetic field lines with the solar
55 wind, known as "opening" magnetic flux, on the dayside boundary of the magnetosphere,
56 or reconnection in the magnetotail on the nightside of the planet which reconnects
57 planetary magnetic field lines to each other, known as "closing" magnetic flux. This should
58 also result in mass loss from the magnetosphere. In a time-averaged sense the outward
59 plasma transport rate should match the plasma loss rate, and the dayside reconnection
60 rate should match that in the magnetotail. Observations of reconnection in the magnetotail
61 can thus provide a method to test the loss process for this internally-produced plasma, as
62 well as the closure of magnetic flux opened on the dayside.

63 Data from the Cassini spacecraft has only provided indirect evidence for reconnection in
64 the magnetotail^{11,12,13,7} and the actual region where magnetic fields are merging, known as
65 the diffusion region, has not been detected at Saturn or Jupiter. The diffusion region has a
66 two-scale structure with the larger ion diffusion region surrounding the smaller electron
67 diffusion region. The ion diffusion region has been detected in observations in Earth's

68 magnetotail^{1,14,15}, Earth's magnetosheath¹⁶, and at Mars^{17,18}. The plasma loss rates
69 inferred from previous observations of magnetic reconnection at Saturn and Jupiter are an
70 order of magnitude too small when compared to the known plasma production rates^{7,19,5}.
71 Here we report the first observations of an ion diffusion region in Saturn's magnetotail.
72 These direct observations show that reconnection can occur over prolonged intervals,
73 almost an order of magnitude longer than the longest previously reported²⁰.

74 Figure 1 shows magnetic field and electron data for a six hour interval on 08 October 2006
75 when Cassini was located in the post-midnight sector of Saturn's magnetosphere around
76 0130 Saturn Local Time, about 8° north of Saturn's equatorial plane, and at a radial
77 distance of 29 R_S, where 1 R_S=60268 km. As illustrated in Figure 2, the magnetic field in
78 the tail is generally in a swept-back into an Archimedean configuration as the result of
79 outward plasma transport and angular momentum conservation. This effect is removed by
80 rotating the data into a new coordinate system where the background magnetic field is in
81 the X direction, and the Y direction is perpendicular to the plane of the swept-back
82 magnetic field (details of the transformation are given in the Supplementary Material). At
83 the beginning of the interval, Cassini was located above the magnetotail current sheet
84 ($B_x > 0$), crossing below ($B_x < 0$) the centre of the current sheet between 03:30 UT – 03:40
85 UT. B_z is ordinarily expected to be negative, as shown in the Supplementary Material. At
86 03:55 UT B_z reverses sign, which in fact corresponds to Cassini crossing the X-line from
87 the tailward to the planetward side as shown in Figure 2. The quantity $|B_z|/\max(|B_x|)$ is an
88 estimate of the reconnection rate and was found to be 0.13 ± 0.10 with a peak of 0.66 –
89 hence consistent with fast magnetic reconnection¹⁶.

90 On the tailward side of the X-line a very energetic (~10 keV/q) ion population is observed
91 flowing tailward, and slightly duskward. This population is not a field-aligned ion beam and
92 has significant perpendicular velocity component. These ions are moving with speeds of

93 1200 km s⁻¹, a substantial fraction of the Alfvén speed of ~4000 km s⁻¹ outside of the
94 current sheet²¹ and much larger than the speed of plasma azimuthally moving around the
95 planet (~150 km s⁻¹), and are identified as the tailward jet from the diffusion region. On the
96 planetward side of the diffusion region the field-of-view of the ion detector does not cover
97 the region where we would expect to see planetward ion beams. Later that day as Cassini
98 leaves the diffusion region the plasma flow returns to near azimuthal motion, but with a
99 tailward and northward component. Detailed analysis of these ion flow directions are
100 presented in the Supplementary Material.

101 Around the magnetic reconnection site ideal magnetohydrodynamics breaks down and
102 charged particles become demagnetised from the magnetic field. Because of a factor of
103 ~1800 in the mass difference between electrons and ions, the ions demagnetise over a
104 larger spatial region than electrons resulting in differential motion between ions and
105 electrons. The resulting current system is known as the Hall current system and produces
106 a characteristic quadrupolar magnetic field structure in the out-of-plane magnetic field, B_y
107 (Figure 2). In the ion diffusion region on the tailward side of the diffusion region B_x and B_y
108 have the same sign but on the planetward side of the X-line B_x and B_y have opposite
109 signs¹⁵. Hence, the sign of B_y can be predicted based on the value of B_x and B_z thus
110 providing a test for the presence of the Hall magnetic field. The red (blue) regions of B_x
111 and B_y in Figure 1 indicate where the B_y component is expected to have a positive
112 (negative) sign associated with this current system and this colour-coding is consistent
113 with the Hall field.

114 As expected, the strength of the Hall field perturbation peaks between the centre and
115 exterior of the current sheet. Three of the four quadrants of the Hall field were measured
116 by Cassini, as indicated by simplified sketch of Cassini's trajectory in Figure 2, based on
117 the data in Figure 1. As calculated in the Supplementary Material, the strength of the Hall

118 field can be estimated by the quantity $|B_y|/\max(|B_x|)$ and the mean value of 0.18 ± 0.15 is
119 somewhat smaller than that observed in other environments although the peak of 0.83 is
120 more consistent with the typical strength, ~ 0.5 , of the Hall field^{1,18}.

121 As shown in the Supplementary Material, further evidence for the detection of the ion
122 diffusion region is cool ~ 100 eV electrons flowing in response to the Hall current system,
123 and hot $\sim 1-10$ keV electrons flowing out of the diffusion region. Small loop-like magnetic
124 field structures at 02:20-03:00 UT and 03:28-03:40 UT also represent evidence for
125 ongoing reconnection. Taken together, the conclusion is that Cassini encountered a
126 tailward moving ion diffusion region in Saturn's magnetotail as sketched in Figure 2.

127 In two-fluid magnetic reconnection theory the size of the ion diffusion region is a multiple of
128 the ion inertial length, c/ω_i , where c is the speed of light in a vacuum and ω_i is the ion
129 plasma frequency given by $(nZ^2e^2/\epsilon_0m_i)^{1/2}$, where n is the ion number density, Z is the ion
130 charge state, e is the fundamental charge, ϵ_0 is the permittivity of free space, and m_i is the
131 ion mass. Using measurements of magnetotail plasma at $30 R_S$ with a plasma number
132 density of $4 - 8 \times 10^4 \text{ m}^{-3}$ and composition²² of $n_{W^+}/n_{H^+} \sim 2$, the mean ion mass is 1.95×10^{-26}
133 kg and the ion inertial length is $3000 - 4000$ km ($0.05 - 0.06 R_S$), hence, the ion diffusion
134 region at Saturn should be $> \sim 0.06 R_S$ (4000 km) in thickness. The lower plasma density in
135 the saturnian system means that the ion diffusion region is an order of magnitude larger
136 than at Earth. Cassini spends over 150 minutes near the reconnection site, which although
137 is longer than ~ 10 minutes at Earth, is not unexpected given the differing size of the
138 diffusion region itself.

139 Plasmoids are loops of magnetic flux produced as part of the reconnection process and
140 they have been used to estimate⁷ magnetic flux closure in the magnetotail by integrating
141 the product of the B_θ component of the magnetic field and the tailward flow speed. This

142 has shown rates of magnetic flux closure between 0.0029 and 0.024 GWb/R_S, where the
143 dimensions include per unit length because the cross-tail length of the diffusion region is
144 unknown and there is no evidence for large reconnection events that extend the full width
145 of the magnetotail.

146 Applying the same argument to the data in the ion diffusion region in Figure 1, between
147 0146 and 0355 UT, and a flow speed of 1200 km s⁻¹, (based on the ion measurements),
148 the reconnected flux is 0.34 GWb R_S⁻¹ over a 2 hour period. This is more than an order of
149 magnitude greater than the largest estimates based on plasmoid observations alone⁷.
150 From changes in the size of Saturn's main auroral oval, changes in open tail flux are
151 typically 5 GWb over a 10-60 hour period²³ but, occasionally, can be much higher (3.5
152 GWb/hour)⁽²⁴⁾. Our observations are entirely consistent with rates of flux closure inferred
153 from auroral observations, requiring only modest ~10% fractions of the tail width to be
154 involved.

155 Estimates of the mass lost per plasmoid can be made by combining the typical tail plasma
156 density of ~10⁴ m⁻³ of 18 amu per ion plasma, with an estimate for the plasmoid volume of
157 10 R_S³, to give 62×10³ kg per plasmoid. Hence, ~200 plasmoids per day (one every ~7
158 minutes) are required to remove the plasma transported outwards from the inner
159 magnetosphere⁵. By scaling our calculated rate of flux closure by the mass per unit
160 magnetic flux²² of ~10⁻³ kg/Wb, we estimate that this releases 3×10⁵ kg R_S⁻¹ or 3×10⁷ kg,
161 three orders of magnitude larger than previous estimates based on plasmoids²⁰. Events of
162 this magnitude every ~4-40 days are required to match a time-averaged mass loading rate
163 of 100 kg/s, rather than every 7 minutes from previous estimates based on indirect
164 observations⁵. Hence, these results demonstrate that magnetotail reconnection can close
165 sufficient amounts of magnetic flux and act as a very significant mass loss mechanism.

166 Additional indirect signatures of magnetic reconnection are also observed two hours after
167 the diffusion region moves tailward. Figure 3 shows five hours of electron fluxes and
168 magnetometer data revealing a series of reconnection signatures in a spherical polar
169 (Kronocentric radial-theta-phi, KRTP) coordinate system. Bipolar perturbations in the B_{θ}
170 component indicate the passage of a loop-like magnetic flux structure and the sense of the
171 perturbation indicates the direction of travel, i.e. a negative-positive perturbation is moving
172 tailward⁷. At 0610 UT a tailward moving loop passes near the spacecraft, sourced from an
173 diffusion region planetward of the spacecraft. At 0705 and 0810 UT a sharp increase in B_{θ}
174 to large positive values is indicative of the compression of magnetic field lines around
175 plasma moving rapidly towards the planet as the result of magnetic reconnection downtail
176 from the spacecraft²⁵. These are known as dipolarisation fronts and they indicate the
177 presence of an diffusion region tailward of the spacecraft. Following the passage of the
178 fronts the spacecraft is immersed in hot plasma, similar to that seen in Earth's
179 magnetotail²⁶, and this is a signature of the energy conversion in the reconnection process.
180 After the final dipolarisation front passes Cassini, the spacecraft is located in a region of
181 fluctuating magnetic fields similar to a chain of magnetic islands (loops) and is surrounded
182 by energetic ~ 10 keV electrons²⁷ which from 0810 to 0910 UT also display evidence of
183 becoming more energetic with time. Ion flows with a planetward component are found
184 throughout this hot plasma region with speeds in excess of ~ 1000 km s⁻¹. Towards the end
185 of the interval, between 15:00 and 17:25 UT, planetward flowing ions and electrons are
186 found in a layer between the centre of the current sheet and its exterior, which are
187 consistent with outflows from a more distant diffusion region²⁸. The detailed particle
188 analysis is presented in the Supplementary Material.

189 These data are evidence for ongoing but time variable magnetic reconnection in the
190 magnetotail at this local time over a period of 19 hours, covering almost two rotations of

191 Saturn. Simulations of upstream solar wind conditions presented in the Supplementary
192 Information show that the magnetosphere was strongly compressed just before the entry
193 into the diffusion region, suggesting triggering of tail reconnection by a solar wind pressure
194 pulse. As shown in the Supplementary Material, a weaker pressure pulse arrives on 09
195 October at 1400 UT when Cassini was located in the inner magnetosphere. Wave
196 signatures suggest that this triggered further reconnection. These observations stand in
197 contrast to the much less frequent plasmoid observations that have previously been used
198 to infer rates of magnetic reconnection in Saturn's magnetotail. At this point it is not
199 possible to determine whether this is a consequence of the magnitude of the solar wind
200 pressure increase, or if this is simply a common event but rarely observed due to the orbit
201 of Cassini and the spatial distribution/spatial size of diffusion regions. These results show
202 that prolonged magnetotail reconnection can close sufficient magnetic flux and shed
203 sufficient mass to explain the time-averaged driving of Saturn's magnetosphere.

204 **References and notes**

- 205 1. Øieroset, M., Phan, T.D., Fujimoto, M., Lin, R.P., Lepping, R.P. In situ detection of
206 collisionless reconnection in the Earth's magnetotail. *Nature* **412**, pp. 414-417 (2001).
- 207 2. Eastwood, J. P. *et al.* Evidence for collisionless magnetic reconnection at Mars.
208 *Geophys. Res. Lett.* **35**, L02106, doi:10.1029/2007GL032289 (2008).
- 209 3. Chen, L.-J. *et al.* Observation of energetic electrons within magnetic islands. *Nature*
210 *Physics* **4**, pp.19-23, doi:10.1038/nphys777, 2008.
- 211 4. Angelopoulos, V. *et al.* Electromagnetic energy conversion at reconnection fronts.
212 *Science* **341**, 1478-1482 (2013).

- 213 5. Bagenal, F. & Delamere, P.A. Flow of mass and energy in the magnetospheres of
214 Jupiter and Saturn. *J. Geophys. Res.* **116**, A05209, doi:10.1029/2010JA016294 (2011).
- 215 6. Thomsen, M.F. Saturn's magnetospheric dynamics. *Geophys. Res. Lett.* **40**,
216 doi:10.1002/2013GL057967 (2013).
- 217 7. Jackman, C.M. *et al.* Saturn's dynamic magnetotail: A comprehensive magnetic field
218 and plasma survey of plasmoids and traveling compression regions and their role in global
219 magnetospheric dynamics. *J. Geophys Res. Space Physics*, **119**, 5465-5495,
220 doi:10.1002/2013JA019388 (2014).
- 221 8. Jurac, S. & Richardson, J. D. A self-consistent model of plasma and neutrals at Saturn:
222 Neutral cloud morphology. *J. Geophys. Res.* **110**, A09220, doi:10.1029/2004JA010635
223 (2005).
- 224 9. Hansen, C. J. *et al.* Enceladus water vapour plume. *Science* **311**(5766), 1422-1425
225 (2006).
- 226 10. Fleshman, B. L., Delamere, P. A., Bagenal, F. A sensitivity study of the Enceladus
227 torus. *J. Geophys. Res.* **115**, E04007, doi:10.1029/2009JE003372, (2010).
- 228 11. Jackman, C. M. *et al.* Strong rapid dipolarizations in Saturn's magnetotail: In situ
229 evidence of reconnection. *Geophys. Res. Lett.* **34**, L11203, doi:10.1029/2007GL029764
230 (2007).
- 231 12. Hill, T. W. *et al.* Plasmoids in Saturn's magnetotail. *J. Geophys. Res.* **113**, A01214,
232 doi:10.1029/2007JA012626 (2008).
- 233 13. Mitchell, D.G. *et al.* Energetic ion acceleration in Saturn's magnetotail: Substorms at
234 Saturn? *Geophys. Res. Lett.* **32**, L20S01 (2005)

- 235 14. Nagai, T. *et al.* Geotail observations of the Hall current system: Evidence of magnetic
236 reconnection in the magnetotail. *J. Geophys. Res.* **106**, A11, pp. 25929-25949 (2001).
- 237 15. Eastwood, J. P., Phan, T. D., Øieroset, M., Shay, M. A. Average properties of the
238 magnetic reconnection ion diffusion region in the Earth's magnetotail: The 2001-2005
239 Cluster observations and comparison with simulations. *J. Geophys. Res.* **115**, A08215,
240 doi:10.1029/2009JA014962 (2010).
- 241 16. Phan, T.D. *et al.* Evidence for magnetic reconnection initiated in the magnetosheath.
242 *Geophys. Res. Lett.* **34**, L14104, doi:10.1029/2007GL030343, 2007.
- 243 17. Eastwood, J. P. *et al.* Evidence for collisionless magnetic reconnection at Mars.
244 *Geophys. Res. Lett.* **35**, L02106, doi:10.1029/2007GL032289 (2008).
- 245 18. Halekas, J. S. *et al.* In situ observations of reconnection Hall magnetic fields at Mars:
246 Evidence for ion diffusion region encounters. *J. Geophys. Res.* **114**, A11204,
247 doi:10.1029/2009JA014544 (2009).
- 248 19. Vogt, M.F. *et al.* Structure and statistical properties of plasmoids in Jupiter's
249 magnetotail. *J. Geophys. Res.* **119**, 821-843, doi:10.1002/2013JA019393 (2014).
- 250 20. Thomsen, M.F., Wilson, R.J., Tokar, R.L., Reisenfeld, D.B., Jackman, C.M.
251 Cassini/CAPS observations of duskside tail dynamics at Saturn. *J. Geophys. Res. Space*
252 *Physics* **118**, 5767-5781, doi:10.1002/jgra.50552, 2013.
- 253 21. Arridge, C. S. *et al.* Plasma electrons in Saturn's magnetotail: Structure, distribution
254 and energisation. *Planet. Space Sci.* **57**, 2032-2047, doi:10.1016/j.pss.2009.09.007 (2009).

- 255 22. McAndrews, H.J. *et al.* Plasma in Saturn's nightside magnetosphere and the
256 implications for global circulation. *Planet. Space Sci.* **57**, pp.1714-1722,
257 doi:10.1016/j.pss.2009.03.003, 2009.
- 258 23. Badman, S.V., Jackman, C.M., Nichols, J.D., Clarke, J.T., Gérard, J.-C. Open flux in
259 Saturn's magnetosphere. *Icarus* **231**, pp.137-145, doi:10.1016/j.icarus.2013.12.004 (2014).
- 260 24. Radioti, A. *et al.* Saturn's elusive nightside polar arc. *Geophys. Res. Lett.* **41**, 6321–
261 6328, doi:10.1002/2014GL061081, 2014.
- 262 25. Runov, A. *et al.* A THEMIS multicas e study of dipolarization fronts in the magnetotail
263 plasma sheet. *J. Geophys. Res.* **116**, A05216, doi:10.1029/2010JA016316, 2011.
- 264 26. Angelopoulos, V. *et al.* Electromagnetic energy conversion at reconnection fronts.
265 *Science* **341**, 1478-1482 (2013).
- 266 27. Chen, L.-J. *et al.* Observation of energetic electrons within magnetic islands. *Nature*
267 *Physics* **4**, pp.19-23, doi:10.1038/nphys777, 2008.
- 268 28. Onsager, T.G., Thomsen, M.F., Gosling, J.T., Bame, S.J. Electron distributions in the
269 plasma sheet boundary layer: Time-of-flight effects. *Geophys. Res. Lett.* **17**, 1837-1840
270 (1990).

271 **Corresponding author**

272 Correspondence and requests for materials should be addressed to C.S. Arridge at
273 c.arridge@lancaster.ac.uk.

274 **Acknowledgements**

275 CSA was funded in this work by a Royal Society Research Fellowship. CMJ was funded
276 by an STFC Ernest Rutherford Fellowship. MFT was supported by the NASA Cassini
277 program through JPL contract 1243218 with Southwest Research Institute and is grateful
278 to Los Alamos National Laboratory for support provided her as a guest scientist. JPE and
279 MKD were supported by STFC grant ST/K001051/1.

280 CSA/CMJ/JAS/NA/XJ/AK/AR/MV/APW acknowledge the support of the International
281 Space Science Institute where part of this work was carried out. Cassini operations are
282 supported by NASA (managed by the Jet Propulsion Laboratory) and ESA. The data
283 reported in this paper are available from the NASA Planetary Data System
284 <http://pds.jpl.nasa.gov/>. SKR data were accessed through the Cassini/RPWS/HFR data
285 server <http://www.lesia.obspm.fr/kronos> developed at the Observatory of Paris/LESIA with
286 support from CNRS and CNES. Solar wind simulation results have been provided by the
287 Community Coordinated Modeling Center at Goddard Space Flight Center through their
288 public Runs on Request system (<http://ccmc.gsfc.nasa.gov>). The CCMC is a multi-agency
289 partnership between NASA, AFMC, AFOSR, AFRL, AFWA, NOAA, NSF and ONR. The
290 ENLIL Model was developed by the D. Odstrcil at the University of Colorado at Boulder.

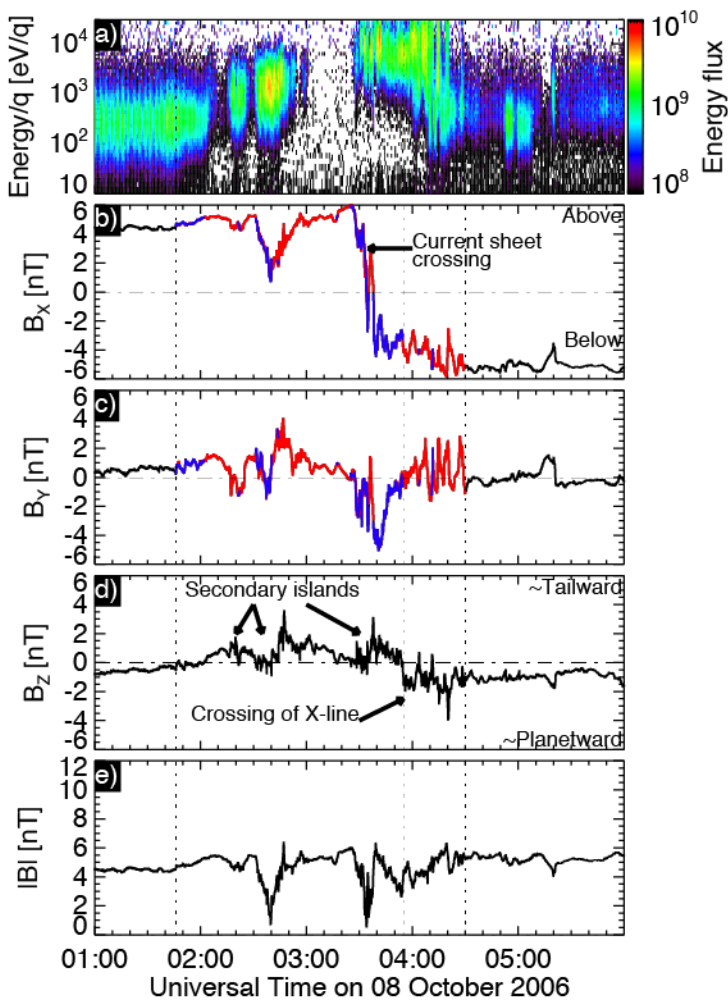
291 **Author Contributions**

292 CSA identified the event in the Cassini data and led the analysis. JPE, CMJ, JAS, GKP,
293 MFT and NS provided detailed assistance with analysis of the magnetic field and particle
294 data. LL and PZ analysed the Cassini radio and plasma wave data and provided an
295 interpretation of the kilometric radiation data. NA, XJ, AK, AR, MV, APW discussed the
296 detailed interpretation of the event with CSA and provided additional expertise to clarify
297 the interpretation and its wider significance. DBR Developed software used to fit CAPS
298 time-of-flight spectra. AJC and MKD provided Cassini CAPS/ELS and MAG and oversaw

299 data processing/science planning. All authors participated in writing the manuscript and
300 the Supplementary Material.

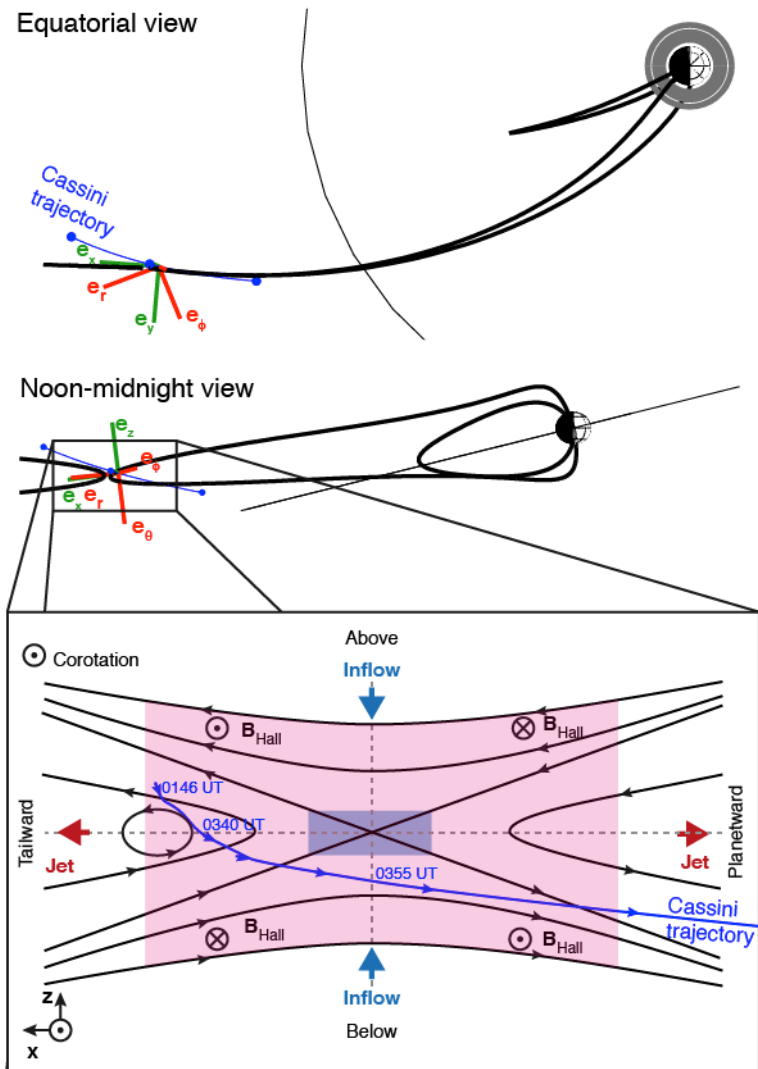
301 **Figure captions**

302 Figure 1: Interval encompassing an ion diffusion region in Saturn's magnetotail as seen by
303 the Cassini spacecraft. Panel (a) electron omnidirectional flux time-energy spectrogram in
304 units of differential energy flux ($\text{eV m}^{-2} \text{sr}^{-1} \text{s}^{-1} \text{eV}^{-1}$); (b-d) three components of the
305 magnetic field in the X-line coordinate system, parts of the B_x and B_y traces in red (blue)
306 show where the B_y component is expected to be positive (negative); (e) the field
307 magnitude.



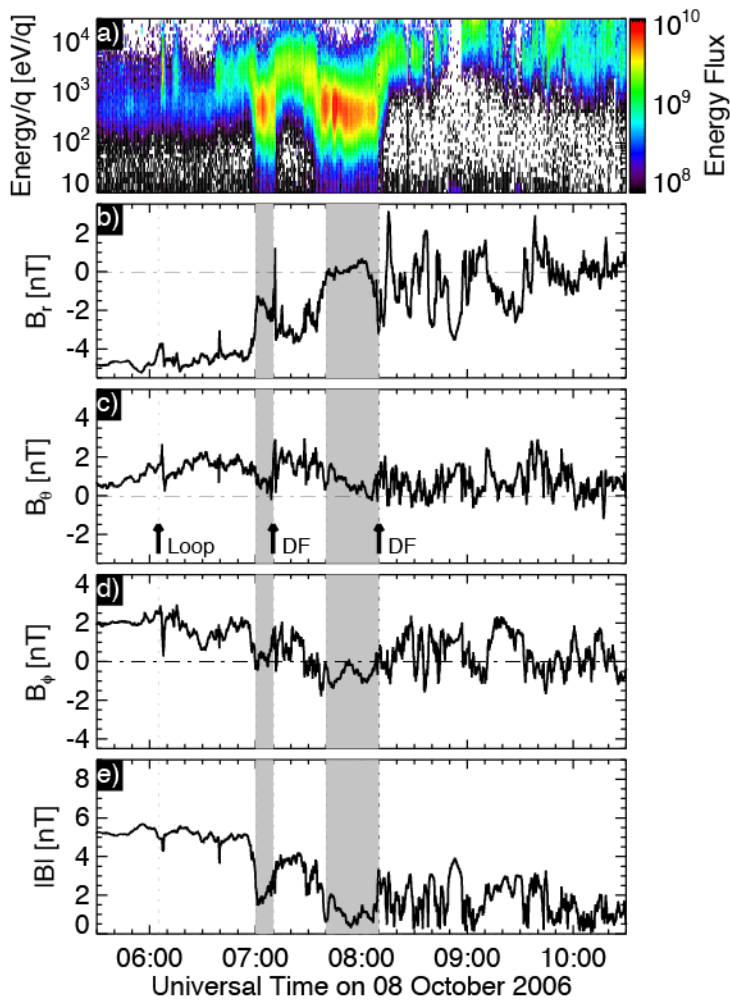
308

309 Figure 2: Geometry of the X-line coordinate system and schematic of Cassini's motion
 310 relative to the X-line. The red vectors show the original spherical polar coordinate system
 311 from the magnetometer data and the green vectors show the new X-line coordinate
 312 system which takes into account the swept-back configuration of the magnetic field. The
 313 blue curve in the top two panels shows the orbit of Cassini around Saturn and in the
 314 bottom view we show a simplified sketch of the inferred motion of Cassini relative to the
 315 magnetic reconnection X-line. The pink and blue regions are the ion and electron diffusion
 316 regions⁹.



317

318 Figure 3: Dipolarisation fronts (DF), magnetic loop (Loop), and the restart of reconnection.
 319 Panel (a) electron omnidirectional flux time-energy spectrogram in units of differential
 320 energy flux ($\text{eV m}^{-2} \text{sr}^{-1} \text{s}^{-1} \text{eV}^{-1}$); (b-d) three components of the magnetic field in spherical
 321 polar coordinates. The grey region indicates periods where the spacecraft is immersed in
 322 the plasma sheet.



323